

Autoignition and detonation development induced by a hot spot in fuel-lean and CO₂ diluted n-heptane/air mixtures

Peng Dai^{a,*}, Zheng Chen^{b,c}, Xiaohua Gan^a

^a Department of Mechanic and Aerospace Engineering, Southern University of Science and Technology, Shenzhen 518055, China

^b SKLTCs, CAPT, College of Engineering, Peking University, Beijing 100871, China

^c Beijing Innovation Center for Engineering Science and Advanced Technology, Peking University, Beijing 100871, China



ARTICLE INFO

Article history:

Received 26 September 2018

Revised 4 November 2018

Accepted 19 December 2018

Keywords:

Autoignition
Detonation development
Fuel-lean
CO₂ dilution
Excitation time
n-heptane

ABSTRACT

Fuel-lean or diluted combustion is widely used in advanced internal combustion engines (ICEs) such as homogeneous charge compression ignition (HCCI) engines, low temperature combustion (LTC) engines, and engines utilizing exhaust gas recirculation (EGR). The thermal efficiency of ICEs is constrained by knock and super-knock due to end-gas autoignition and detonation development. Therefore, the effects of equivalence ratio and CO₂ dilution on autoignition and detonation development induced by a hot spot are numerically investigated here. It is found that the decrease of equivalence ratio and increase of CO₂ dilution ratio can both greatly increase the excitation time and reduce the total heat release. Under fuel-leaner or more diluted conditions, the interaction between chemical reaction and pressure wave becomes weaker and thereby the propensity of detonation development is lower. Different autoignition modes are identified and quantified. The excitation time is shown to play a controlling role in the chemical-acoustic interaction and detonation development. It is demonstrated that reducing equivalence ratio and increasing CO₂ dilution have the same influence on the autoignition mode if the same excitation time is maintained. Furthermore, the detonation development regimes for n-heptane and dimethyl ether at different conditions are obtained and compared. Non-dimensional parameters used to well quantify the detonation development regime are identified and discussed.

© 2018 The Combustion Institute. Published by Elsevier Inc. All rights reserved.

1. Introduction

Recently, downsizing of spark-ignition engines (SIEs) utilizing highly boosting technologies such as turbocharging has become a popular way to improve thermal efficiency. However, propensity of knock and super-knock increases greatly in SIEs under boosted environment [1–5], especially in low-speed and high-load condition. This brings the major challenge for developing engines with high efficiency. It is generally accepted that conventional knock in SIEs originates from end-gas autoignition, while the intensive chemical-acoustic interaction and detonation development induced by localized hot spot are the major cause of super-knock [6–9]. On the other hand, fuel-lean and low-temperature combustion has the advantage of reducing both NO_x emission and fuel consumption [10–14], and it is used in advanced engines such as homogeneous charge compression ignition (HCCI) engines, low temperature combustion (LTC) engines, and engines utilizing exhaust gas recirculation (EGR). During the combustion process in these engines,

reactivity non-uniformity is inevitable which might induce detonation development [9,15]. Therefore, fundamental understanding of end-gas autoignition and detonation development induced by reactivity non-uniformity under fuel-lean or diluted condition is needed.

According to the reactivity gradient theory of Zel'dovich [16,17], different autoignition modes including detonation development may be induced by a hot spot. The theory was confirmed by simulations considering simplified [18–23] or detailed chemical mechanisms [24–33]. Among them, Bradley and co-workers [25,26] identified a detonation peninsular based on two non-dimensional parameters: the normalized temperature gradient, ξ , and the ratio of acoustic time to excitation time, ε . This detonation peninsular was then widely used in studies related to engine knock [3,6–8,34–44]. For examples, Bates et al. [37] quantitatively analyzed different engine conditions corresponding to regimes from benign autoignition to super-knock by utilizing the ξ - ε diagram; Robert et al. [8] investigated various scenarios for knock and super-knock by using LES and the ξ - ε diagram; and in our work [30–32] detonation development regimes were identified in ξ - ε diagram for large hydrocarbons with low-temperature chemistry. More recently, we have introduced a new non-dimensional parameter, ξ_a ,

* Corresponding author.

E-mail address: daip@sustc.edu.cn (P. Dai).

to quantify regimes of different autoignition modes [33]. The new parameter ξ_a is based on the transient autoignition front propagation speed and it is more suitable in describing different autoignition modes [33]. Besides, Yu et al. [45,46], Terashima et al. [47,48] and Wei and co-workers [41,49–51] studied the interaction between flame propagation and end-gas autoignition.

However, stoichiometric fuel/air mixtures were considered in most of previous studies; and there are few studies on detonation development due to reactivity gradient in fuel-lean or diluted mixtures [25,44,52]. For fuel-leaner or more diluted mixtures, the excitation time becomes longer and the volumetric energy density is lower. Consequently, the pressure wave intensity, the interaction between pressure wave and chemical reaction, and the propensity of detonation should depend on the equivalence ratio and dilution. Therefore, the objectives of this study are to assess and interpret the effects of equivalence ratio and CO₂ dilution on autoignition and detonation development induced by a hot spot in n-heptane/air mixture and to assess the performance of different parameters in terms of quantitatively describing autoignition modes under different conditions.

2. Numerical model and methodologies

The transient autoignition front propagation process initiated by a hot spot at the center of a 1-D, adiabatic, closed, spherical chamber is investigated in this study. The hot spot is characterized by a linear temperature distribution with negative gradient:

$$T_i(r) = \begin{cases} T_{i,0} + (r - r_0)(dT/dr)_i & (r \leq r_0) \\ T_{i,0} = 1000 \text{ K} & (r_0 < r \leq R_w) \end{cases} \quad (1)$$

where r is radial spatial coordinate; r_0 is the hot spot radius varying from 1 to 8 mm which is representative for length scale of thermal stratification; $R_w = 4$ cm is the radius of the spherical chamber; $(dT/dr)_i$ is the specified temperature gradient within the hot spot, and $T_{i,0} = 1000$ K is the initial temperature outside of the hot spot. The initial n-heptane/air/CO₂ mixture composition is uniform in the chamber with specified equivalence ratio, ϕ , and CO₂ dilution ratio, c_{CO_2} . The mixture is initially static (i.e., $u = 0$ m/s) at $P_0 = 40$ atm.

The skeletal mechanism for n-heptane oxidation [53] consisting of 44 species and 112 elementary reactions is used in simulation. It has been demonstrated to be able to accurately predict ignition and flame propagation in n-heptane/air mixture at a broad range of temperature, pressure and equivalence ratio [53]. It is noted that compared to the detailed mechanism, the skeletal mechanism can accurately predict the ignition delay time, while there are large discrepancies in the excitation time (see Fig. S2 in the Supplemental Material). In fact, it is difficult to measure the excitation time in experiments; and both detailed and skeletal mechanisms were not validated against experiments in terms of excitation time. This deserves further study, which is beyond the scope of the current work. Moreover, the skeletal mechanism was not validated for CO₂ diluted mixtures. Nevertheless, the effects of CO₂ dilution on the ignition delay and excitation times are at least qualitatively predicted by the skeletal mechanism.

The transient autoignition process is simulated using the in-house code A-SURF (Adaptive Simulation of Unsteady Reactive Flow) [29,54,55] which solves the conservation equations for 1-D, adiabatic, multi-component, reactive flow using finite volume method. A multi-level, dynamically adaptive mesh refinement algorithm [56,57] is used to ensure adequate numerical resolution of the reaction zone, pressure wave, shock wave, and detonation wave [54,55], which are always covered by the finest mesh with 1.56 μm in width. The time step is 0.312 ns. Details on the numerical model, governing equations, numerical scheme, and grid convergence are provided in Section S1 of the Supplemental Material.

3. Results and discussion

3.1. 0-D homogeneous ignition

0-D homogeneous ignition of n-heptane/air/CO₂ mixture at constant volume is first investigated. The ignition delay time, τ , is defined as the time for maximum heat release rate. The excitation time, τ_e , evaluates the rapidity of major ignition heat release, and it is defined as the time interval between 5% and maximum heat release rate [26]. Figure 1 shows the influence of equivalence ratio and CO₂ dilution on τ and τ_e at $T_0 = 1000$ K and $P_0 = 40$ atm. Both τ and τ_e increase with decreasing ϕ or increasing c_{CO_2} . However, compared to τ , τ_e is much more sensitive to ϕ and c_{CO_2} . The excitation time can be enlarged by 100 times through reducing the equivalence ratio or increasing the CO₂ dilution. This indicates that the heat release process can be significantly mitigated under fuel-leaner or more diluted condition. Similar trend can be observed for other initial temperature as shown by Fig. S4 in the Supplemental Material.

According to the theory of Zel'dovich [17] and Gu et al. [26], there is a critical temperature gradient at which the theoretical autoignition front propagation speed, u_a , is equal to the sound speed, a . This critical temperature gradient is defined as [26]:

$$(dT/dr)_c = (a(d\tau/dT_0))^{-1} \quad (2)$$

where $d\tau/dT_0$ can be obtained from 0-D ignition simulation. The critical temperature gradient is also plotted in Fig. 1. It is observed that the critical temperature gradient can be reduced by 50% through reducing the equivalence ratio or increasing the CO₂ dilution. This also indicates that the autoignition mode may change when the mixture becomes fuel-leaner or more diluted.

At fuel-leaner or higher CO₂ diluted condition, the volumetric energy density becomes lower. Figure 2 shows that with the decrease of equivalence ratio or increase of CO₂ dilution, the excitation time becomes longer and the volumetric energy density is lower. Consequently, it is expected that the pressure wave and its interaction with chemical reaction both become weaker and thereby the propensity of detonation development becomes lower. This will be demonstrated in the next subsection.

3.2. 1-D autoignition with hot spot

The autoignition front propagation process induced by a hot spot is simulated at different fuel-lean or CO₂ diluted conditions. The normalized temperature gradient of the hot spot, ξ , is defined as [26]:

$$\xi = (dT/dr)_i / (dT/dr)_{c,r_0/2} \quad (3)$$

where $(dT/dr)_i$ is the specified temperature gradient within the hot spot (see Eq. (1)); the subscript $r_0/2$ denotes that the value of critical temperature gradient is evaluated at $r = r_0/2$ in order to represent the average condition within the hot spot [26]. The theoretical autoignition front propagation speed, u_a , can therefore be calculated by ξ through [26]:

$$u_a = a/\xi \quad (4)$$

It is noted that u_a usually differs from the actual transient autoignition front propagation speed, denoted as S , due to the impact of thermal/mass diffusion transport around the hot spot during induction period. Therefore, in Ref. [33] we introduced another non-dimensional parameter, ξ_a , based on the actual autoignition front propagation speed:

$$\xi_a = a_{r_0/2}/S_{AVG} \quad (5)$$

where $a_{r_0/2}$ and S_{AVG} are respectively the sound speed at $r = r_0/2$ and the average speed of autoignition front propagating within the hot spot (i.e., $0 \leq r \leq r_0$) calculated from 1-D simulation. It was

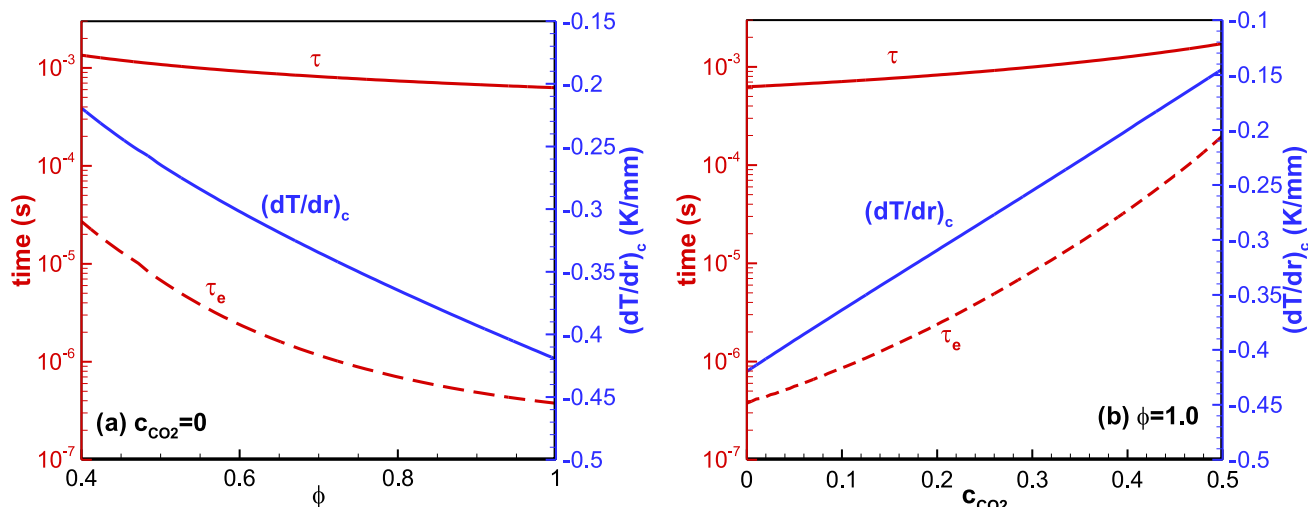


Fig. 1. Change of 0-D ignition delay time, excitation time and critical temperature gradient with (a) equivalence ratio (without CO₂ dilution, i.e., $c_{CO_2} = 0$) and (b) CO₂ molar fraction (for stoichiometric mixture with $\phi = 1$) in n-heptane/air/CO₂ mixture at $T_0 = 1000$ K and $P_0 = 40$ atm.

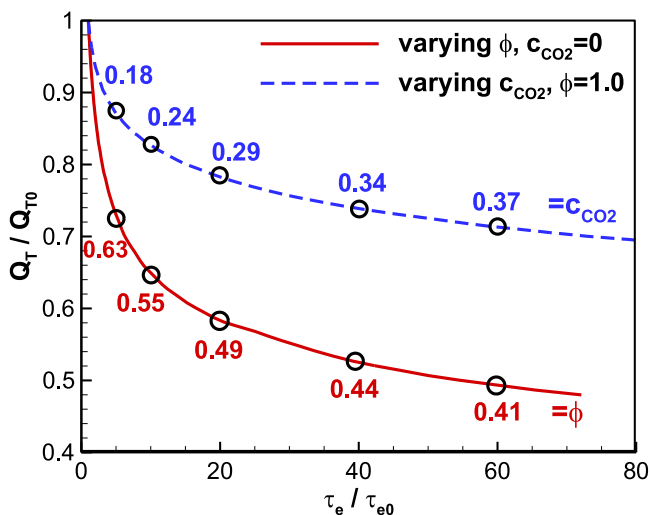


Fig. 2. Change of total heat release during 0-D ignition with the corresponding excitation time, which are respectively normalized by the values of undiluted stoichiometric mixture (i.e., Q_{T0} and τ_{e0} at $\phi = 1.0$ and $c_{CO_2} = 0$). The initial temperature and pressure are respectively $T_0 = 1000$ K and $P_0 = 40$ atm.

demonstrated that ξ_a increases monotonously with ξ and that the detonation development regime can be better quantified in the ξ_a - ε diagram than in the ξ - ε diagram [33].

The influences of equivalence ratio and CO₂ dilution on autoignition process are investigated by considering n-heptane/air without CO₂ dilution (i.e., $\phi \leq 1.0$, $c_{CO_2} = 0$) and stoichiometric n-heptane/air with different amounts of CO₂ dilution (i.e., $\phi = 1.0$, $c_{CO_2} \geq 0$), respectively. Details of the simulated cases are summarized in Figs. S6–S8 in the Supplemental Material. Only the autoignition modes are summarized and shown in Fig. 3 for three hot spot sizes of $r_0 = 2, 3.5$ and 5 mm. For each hot spot size, three autoignition modes can be sequentially identified with the increase of ξ_a , namely: (I) supersonic reaction front propagation, (II) detonation development, and (III) subsonic reaction front propagation. Figure 3(a) shows that the detonation development mode is located within a C-shaped curve in the ξ_a - ϕ diagram. As expected, the propensity of detonation development induced by a hot spot is reduced in fuel-leaner mixture. Under very lean condition (e.g., $\phi \leq 0.6$ at $r_0 = 5$ mm), detonation development cannot be

observed. Therefore, detonation development and super-knock can be prevented in ICES using ultra-lean combustion. Similarly, Fig. 3(b) indicates that detonation development and super-knock become more difficult at higher CO₂ dilution and they can be prevented when high EGR is used. Figure 3 also shows that the detonation development regime is narrower for smaller hot spot size, implying that it is more difficult to achieve detonation development for a smaller hot spot. This is mainly because the total chemical energy deposited into the developing pressure wave within the hot spot is reduced as r_0 decreases [26,30].

In order to further reveal the effects of equivalence ratio and CO₂ dilution as well as the hot spot size on autoignition modes, four typical autoignition cases, i.e., cases A–D, are analyzed. Case A is chosen for reference ($\phi = 1.0$, $c_{CO_2} = 0$, $r_0 = 5$ mm); and cases B, C, and D respectively reduces equivalence ratio ($\phi = 0.6$, $c_{CO_2} = 0$, $r_0 = 5$ mm), increases CO₂ dilution ($\phi = 1.0$, $c_{CO_2} = 0.2$, $r_0 = 5$ mm), and reduces hot spot size ($\phi = 1.0$, $c_{CO_2} = 0$, $r_0 = 2$ mm). The temperature gradients for these four cases are specified in order to achieve the same value of $\xi_a = 1.5$ (i.e., cases A, B, C, and D are on the same horizontal line as marked in Fig. 3). In addition, cases B and C have the same excitation time of $\tau_e = 2.4$ μ s. Parameters corresponding to these four cases are summarized in Table S1 in the Supplemental Material.

Figure 4 shows the temporal evolution of pressure distribution for these four cases (more details are shown in Figs. S9–S12 in the Supplemental Material). Among these four cases, case A is identified as detonation development mode, while cases B, C and D all correspond to subsonic reaction front propagation mode. It is noted that the same value of ξ_a for these four cases leads to very close reaction front propagation speed within the hot spot, which essentially excludes the influence of transient reaction front propagation within the hot spot. Therefore, the change of autoignition modes in these four cases is mainly due to the modified mixture composition and hot spot size. On the other hand, the autoignition processes for cases B and C which share the same value of τ_e are quite similar to each other. This indicates that reducing equivalence ratio and increasing CO₂ dilution have the same influence on the autoignition mode if the same excitation time is maintained.

To further demonstrate the effect of excitation time on autoignition process, Fig. 5 plots the normalized maximum pressure against normalized excitation time. It is noted that by normalizing the maximum pressure by corresponding equilibrium value of 0-D constant-volume ignition, the effect of total reaction heat

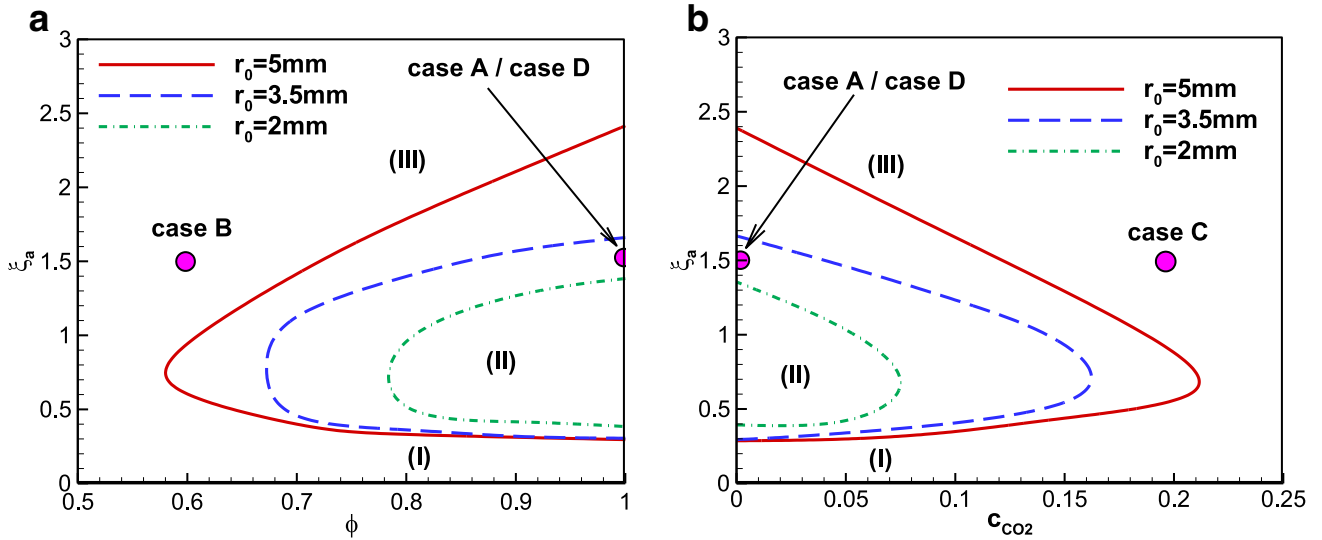


Fig. 3. Regimes of autoignition modes induced by a hot spot with different radii in (a) undiluted n-heptane/air with different equivalence ratios and (b) stoichiometric n-heptane/air with different amounts of CO₂ dilution. Three autoignition modes are (I) supersonic reaction front propagation, (II) detonation development, and (III) subsonic reaction front propagation, respectively.

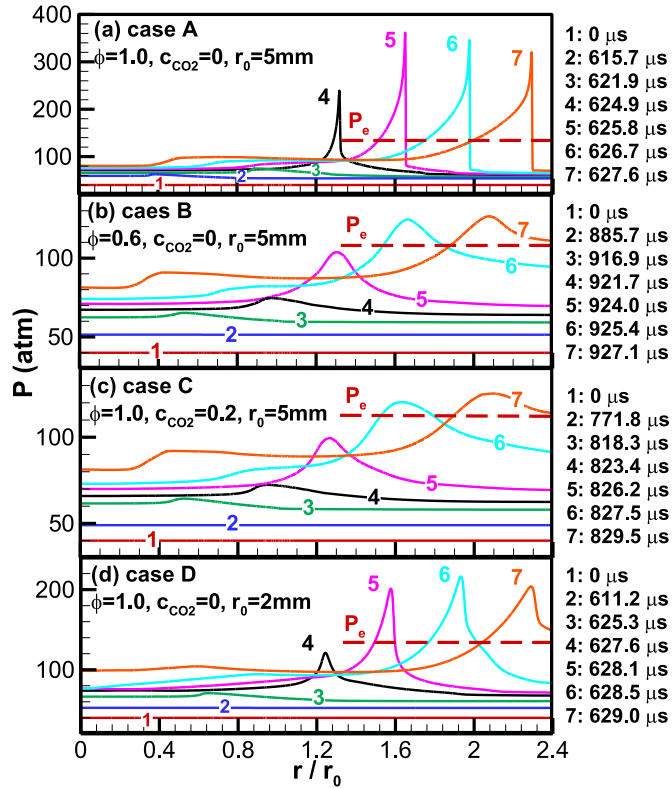


Fig. 4. Temporal evolution of pressure distribution during autoignition with a hot spot for cases A to D. The horizontal dashed line in each sub-figure denotes the corresponding equilibrium pressure of 0-D constant-volume ignition, namely: (a) $P_e = 134$ atm, (b) $P_e = 108$ atm, (c) $P_e = 112$ atm, (d) $P_e = 134$ atm.

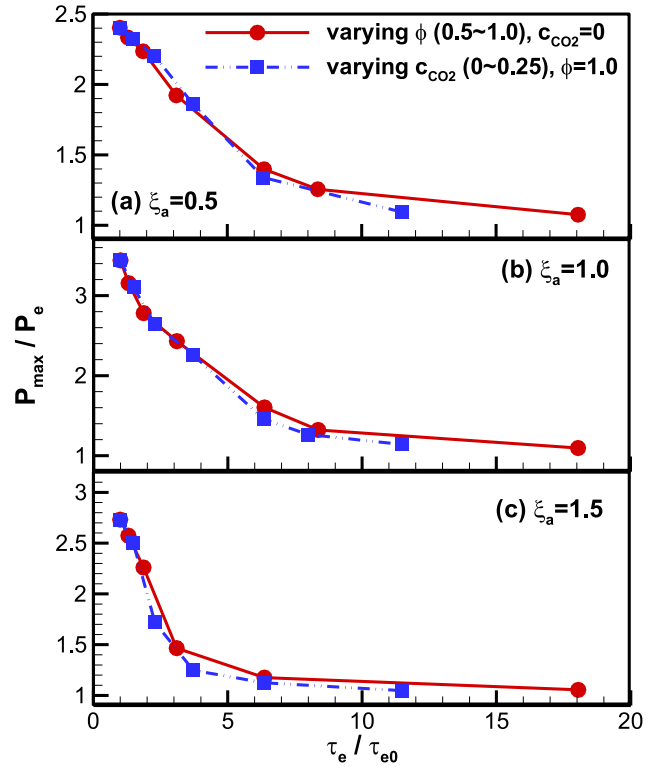


Fig. 5. Change of the maximum pressure, P_{max} , normalized by the equilibrium value of 0-D constant-volume ignition, P_e , with excitation time, τ_e , normalized by the value in undiluted stoichiometric mixture, τ_{e0} , under undiluted fuel-lean or CO₂ diluted stoichiometric conditions. The hot spot size is $r_0 = 5$ mm.

release is excluded. Figure 5 indicates that the excitation time plays a dominating role in the chemical-acoustic interaction process during autoignition. Besides, the results for fuel-lean mixtures with $c_{CO_2} = 0$ are shown to overlap with those for CO₂ diluted mixtures with $\phi = 1$. This further demonstrates that change in equivalence ratio and change in CO₂ dilution can have the same

influence on the autoignition mode if the same excitation time is maintained.

Based on the above discussion, Fig. 6 plots the regimes of three autoignition modes in a $\xi_a - \tau_e / \tau_{e0}$ diagram. The detonation development regime, II, lies within a reversed C-shaped curve in $\xi_a - \tau_e / \tau_{e0}$ diagram. The results at fuel-lean and CO₂ diluted conditions quantitatively agree with each other for a specified hot spot size.

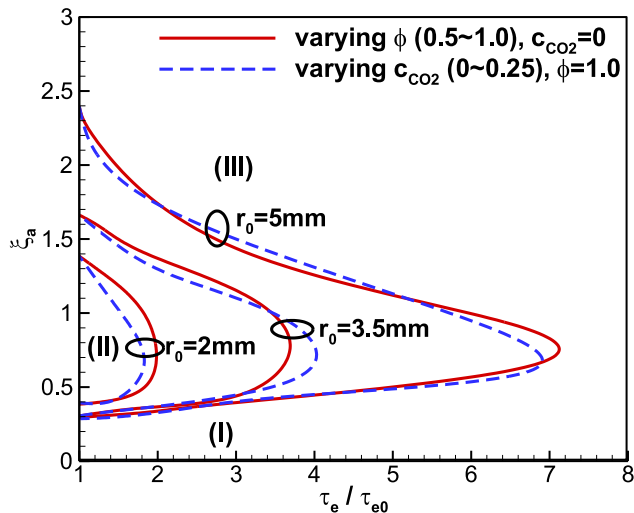


Fig. 6. Regimes of autoignition modes induced by a hot spot in n-heptane/air mixtures under undiluted fuel-lean condition (solid lines) and CO₂ diluted stoichiometric condition (dashed lines).

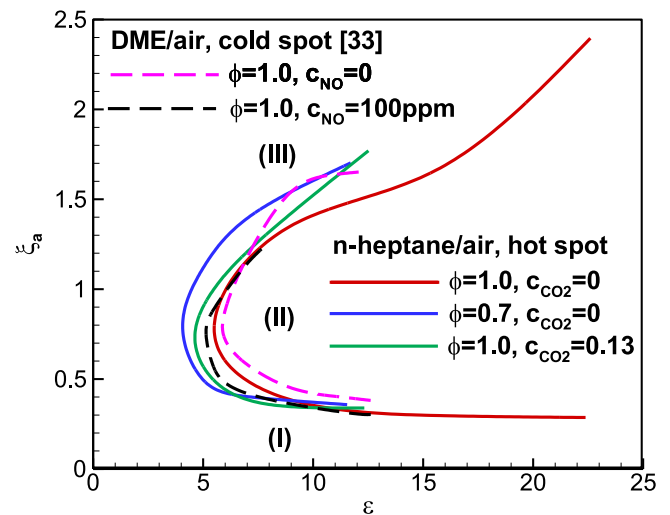


Fig. 8. Regimes of autoignition modes induced by a hot spot in n-heptane/air/CO₂ mixtures at $T_{i,0} = 1000$ K and $P_0 = 40$ atm and by a cold spot in DME/air/NO mixtures at $T_{i,0} = 975$ K and $P_0 = 40$ atm (from Ref. [33]) in ξ_a - ε diagram.

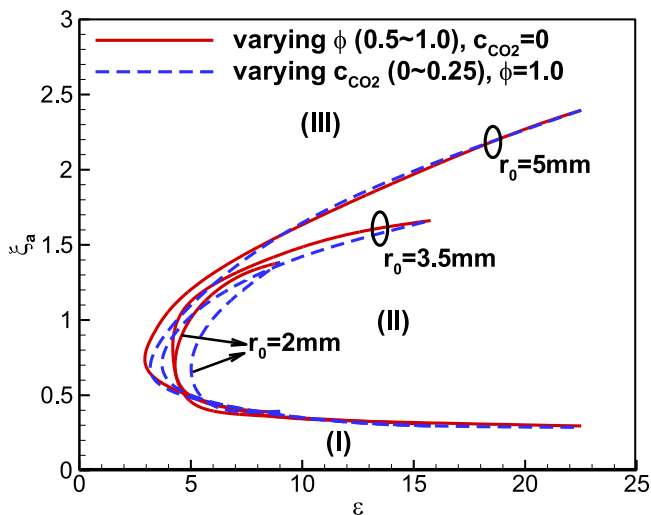


Fig. 7. Regimes of autoignition modes induced by a hot spot with different radii in fuel-lean (solid lines) or CO₂ diluted (dashed lines) n-heptane/air mixtures.

Therefore, for both fuel-lean and CO₂ diluted mixtures, the detonation development regime can be quantified by ξ_a and τ_e/τ_{e0} .

In the ξ_a - τ_e/τ_{e0} diagram in Fig. 6, the effects of hot spot size are clearly demonstrated. The ratio between the acoustic time, r_0/a , and excitation time, τ_e , is then introduced as $\varepsilon = r_0/(a\tau_e)$ [26] and all the results are plotted in the ξ_a - ε diagram as shown in Fig. 7. The detonation development limits indicated by the C-shaped curves are observed to be almost unaffected by the initial condition (including r_0). This indicates that ε can well quantify different autoignition modes by comprehensively assessing the impact of chemical energy deposition into developing pressure wave within the hot spot.

All the above-mentioned detonation limits are obtained by changing the mixture composition (i.e. varying either the equivalence ratio or the CO₂ concentration) at a specified hot spot size. Detonation limits in terms of varying hot spot size (i.e. $r_0 = 1$ –8 mm) at specified mixture compositions are also identified (details are shown in Section S3.5 of the Supplemental Material); and the results are plotted in Fig. 8.

Three mixture compositions are considered, namely the undiluted stoichiometric mixture ($\phi = 1.0$, $c_{\text{CO}_2} = 0$), undiluted

fuel-lean mixture ($\phi = 0.7$, $c_{\text{CO}_2} = 0$), and diluted stoichiometric mixture ($\phi = 1.0$, $c_{\text{CO}_2} = 0.13$). The latter two compositions are chosen since they have the same excitation time of $\tau_e = 1.2$ μs which is much longer than $\tau_e = 0.38$ μs for the undiluted stoichiometric mixture. Therefore, as shown in Fig. 8, in the range of r_0 considered in this study, the detonation limit can be identified at much larger ε for undiluted stoichiometric mixture (i.e. $\varepsilon \approx 22$ at $r_0 = 5$ mm) than the fuel-lean and CO₂ diluted mixtures (i.e. $\varepsilon \approx 12$ at $r_0 = 8$ mm). Moreover, limits of detonation development regime induced by cold spot in dimethyl ether (DME)/air mixture with NO addition from Ref. [33] are also plotted together for comparison. It is seen that the detonation limits for different mixture compositions and initial conditions quantitatively agree with one another in the ξ_a - ε diagram while there are obvious discrepancies among those in ξ - ε diagram (see Fig. S15 in the Supplemental Material, also see Fig. 6 in Ref. [33] and Fig. 3 in Ref. [31]). Therefore, parameter ξ_a is better than ξ in terms of quantifying detonation development regime. However, considering the expensive 1-D simulation required to evaluate ξ_a , ξ_a cannot readily replace ξ in predicting autoignition modes for practical application, but rather complement ξ for better quantitative analysis. Further investigation on the relationship between ξ_a and ξ under different conditions is needed. Furthermore, Fig. 8 shows that the low-temperature chemistry (i.e. in cases with cold spot for DME/air) has negligible effect on the detonation development regime in the ξ_a - ε diagram. This is mainly due to the fact that the reaction front propagation is driven by the main portion of heat release at high temperatures and that low-temperature chemistry only has secondary influence on the chemical-acoustic interaction.

The detonation development regimes for n-heptane/air/CO₂ mixtures shown in Fig. 8 are also compared with those in Fig. 7 (see Fig. S16 in the Supplemental Material). It is found that the regime diagrams identified by varying equivalence ratio, CO₂ concentration, and hot spot size at various conditions quantitatively agree with one another in ξ_a - ε diagram. This indicates that the main physical-chemical factors affecting autoignition process can be adequately represented by the two parameters, ξ_a and ε .

4. Conclusions

Numerical simulation considering detailed chemistry and transport is conducted to study the effects of equivalence ratio and CO₂ dilution on autoignition modes induced by a hot spot in

n-heptane/air mixture. It is found that the decrease of equivalence ratio or increase of CO₂ dilution can greatly increase the excitation time and reduce total ignition heat release (or volumetric energy density). 1-D autoignition front propagation induced by a hot spot under fuel-lean or CO₂ diluted condition is systematically investigated. Three typical autoignition modes are identified, namely (I) supersonic reaction front propagation, (II) detonation development, and (III) subsonic reaction front propagation. The ξ_a - ϕ diagram and ξ_a -cCO₂ diagram are introduced to quantitatively assess the effects of equivalence ratio and CO₂ dilution on autoignition modes. With the decrease of equivalence ratio or increase of CO₂ dilution, the propensity of detonation development becomes lower since the pressure wave and its interaction with chemical reaction both become weaker. Furthermore, the excitation time is found to play a controlling role in the chemical-acoustic interaction during autoignition. Reducing equivalence ratio and increasing CO₂ dilution can have the same influence on the autoignition mode if the same excitation time is kept. Autoignition regimes induced by a hot spot in n-heptane/air/CO₂ mixtures which are obtained by varying equivalence ratio, CO₂ concentration or hot spot size, and those induced by a cold spot in DME/air/NO mixtures [33] are compared in ξ_a - ε diagram. The corresponding detonation development regimes are observed to quantitatively agree with one another under various conditions, indicating that the main physical-chemical factors affecting autoignition process can be adequately represented by ξ_a and ε .

Acknowledgments

This work is supported by National Natural Science Foundation of China (Nos. 51606091 and 91741126). We appreciate helpful discussions with Professor Xiaolong Gou at Chongqing University.

Supplementary materials

Supplementary material associated with this article can be found, in the online version, at doi:10.1016/j.combustflame.2018.12.020.

References

- [1] Z. Wang, H. Liu, T. Song, Y.L. Qi, X. He, S.J. Shuai, J.X. Wang, Relationship between super-knock and pre-ignition, *Int. J. Engine Res.* 16 (2015) 166–180.
- [2] Z. Wang, H. Liu, R.D. Reitz, Knocking combustion in spark-ignition engines, *Prog. Energy Combust. Sci.* 61 (2017) 78–112.
- [3] G. Kalghatgi, Knock onset, knock intensity, superknock and preignition in spark ignition engines, *Int. J. Engine Res.* 19 (2018) 7–20.
- [4] Y.L. Qi, Z. Wang, J.X. Wang, X. He, Effects of thermodynamic conditions on the end gas combustion mode associated with engine knock, *Combust. Flame* 162 (2015) 4119–4128.
- [5] M. Jaasim, E.-A. Tingas, F.E.H. Perez, H.G. Im, Computational singular perturbation analysis of super-knock in SI engines, *Fuel* 225 (2018) 184–191.
- [6] G.T. Kalghatgi, D. Bradley, Pre-ignition and 'super-knock' in turbo-charged spark-ignition engines, *Int. J. Engine Res.* 13 (2012) 399–414.
- [7] J. Rudloff, J.M. Zaccardi, S. Richard, J.M. Anderlohr, Analysis of pre-ignition in highly charged SI engines: emphasis on the auto-ignition mode, *Proc. Combust. Inst.* 34 (2013) 2959–2967.
- [8] A. Robert, S. Richard, O. Colin, T. Poinso, LES study of deflagration to detonation mechanisms in a downsized spark ignition engine, *Combust. Flame* 162 (2015) 2788–2807.
- [9] Z. Wang, Y. Qi, X. He, J. Wang, S. Shuai, C.K. Law, Analysis of pre-ignition to super-knock: hotspot-induced deflagration to detonation, *Fuel* 144 (2015) 222–227.
- [10] T. Li, T. Yin, B. Wang, A phenomenological model of knock intensity in spark-ignition engines, *Energy Convers. Manag.* 148 (2017) 1233–1247.
- [11] Y. Putrasari, N. Jamsran, O. Lim, An investigation on the DME HCCI autoignition under EGR and boosted operation, *Fuel* 200 (2017) 447–457.
- [12] K. Cung, A.A. Moiz, X.C. Zhu, S.Y. Lee, Ignition and formaldehyde formation in dimethyl ether (DME) reacting spray under various EGR levels, *Proc. Combust. Inst.* 36 (2017) 3605–3612.
- [13] H.A. El-Asrag, Y.G. Ju, Direct numerical simulations of NO_x effect on multistage autoignition of DME/air mixture in the negative temperature coefficient regime for stratified HCCI engine conditions, *Combust. Flame* 161 (2014) 256–269.
- [14] J.E. Dec, Advanced compression-ignition engines—understanding the in-cylinder processes, *Proc. Combust. Inst.* 32 (2009) 2727–2742.
- [15] J. Nygren, J. Hult, M. Richter, M. Alden, M. Christensen, A. Hultqvist, B. Johansson, Three-dimensional laser induced fluorescence of fuel distributions in an HCCI engine, *Proc. Combust. Inst.* 29 (2002) 679–685.
- [16] Y.B. Zeldovich, V.B. Librovich, G.M. Makhviladze, G.I. Sivashinsky, On the development of detonation in non-uniformly preheated gas, *Acta Astronaut.* 15 (1970) 313–321.
- [17] Y.B. Zeldovich, Regime classification of an exothermic reaction with nonuniform initial conditions, *Combust. Flame* 39 (1980) 211–214.
- [18] J.F. Clarke, Fast flames, waves and detonation, *Prog. Energy Combust. Sci.* 15 (1989) 241–271.
- [19] A.M. Khokhlov, E.S. Oran, J.C. Wheeler, A theory of deflagration-to-detonation transition in unconfined flames, *Combust. Flame* 108 (1997) 503–517.
- [20] A.K. Kapila, D.W. Schwendeman, J.J. Quirk, T. Hawa, Mechanisms of detonation formation due to a temperature gradient, *Combust. Theory Model.* 6 (2002) 553–594.
- [21] G.J. Sharpe, M. Short, Detonation ignition from a temperature gradient for a two-step chain-branching kinetics model, *J. Fluid Mech.* 476 (2003) 267–292.
- [22] M.D. Kurtz, J.D. Regele, Acoustic timescale characterisation of a one-dimensional model hot spot, *Combust. Theory Model.* 18 (2014) 532–551.
- [23] A. Misdariis, O. Vermorel, T. Poinso, A methodology based on reduced schemes to compute autoignition and propagation in internal combustion engines, *Proc. Combust. Inst.* 35 (2015) 3001–3008.
- [24] H.J. Weber, A. Mack, P. Roth, Combustion and pressure wave interaction in enclosed mixtures initiated by temperature nonuniformities, *Combust. Flame* 97 (1994) 281–295.
- [25] D. Bradley, C. Morley, X.J. Gu, D.R. Emerson, Amplified pressure waves during autoignition: relevance to CAI engines, *SAE Technical Paper* 2002-01-2868 (2002).
- [26] X.J. Gu, D.R. Emerson, D. Bradley, Modes of reaction front propagation from hot spots, *Combust. Flame* 133 (2003) 63–74.
- [27] M.A. Liberman, A.D. Kiverin, M.F. Ivanov, On detonation initiation by a temperature gradient for a detailed chemical reaction models, *Phys. Lett. A* 375 (2011) 1803–1808.
- [28] M.A. Liberman, A.D. Kiverin, M.F. Ivanov, Regimes of chemical reaction waves initiated by nonuniform initial conditions for detailed chemical reaction models, *Phys. Rev. E* 85 (2012) 056312.
- [29] P. Dai, Z. Chen, Supersonic reaction front propagation initiated by a hot spot in n-heptane/air mixture with multistage ignition, *Combust. Flame* 162 (2015) 4183–4193.
- [30] P. Dai, Z. Chen, S.Y. Chen, Y.G. Ju, Numerical experiments on reaction front propagation in n-heptane/air mixture with temperature gradient, *Proc. Combust. Inst.* 35 (2015) 3045–3052.
- [31] P. Dai, C.K. Qi, Z. Chen, Effects of initial temperature on autoignition and detonation development in dimethyl ether/air mixtures with temperature gradient, *Proc. Combust. Inst.* 36 (2017) 3643–3650.
- [32] C.K. Qi, P. Dai, H. Yu, Z. Chen, Different modes of reaction front propagation in n-heptane/air mixture with concentration non-uniformity, *Proc. Combust. Inst.* 36 (2017) 3633–3641.
- [33] P. Dai, Z. Chen, Effects of NO_x addition on autoignition and detonation development in DME/air under engine-relevant conditions, *Proc. Combust. Inst.* 37 (2018) Submitted for publication, doi:10.1016/j.proci.2018.06.063.
- [34] D. Bradley, G.T. Kalghatgi, Influence of autoignition delay time characteristics of different fuels on pressure waves and knock in reciprocating engines, *Combust. Flame* 156 (2009) 2307–2318.
- [35] D. Bradley, Autoignitions and detonations in engines and ducts, *Philos. Trans. R. Soc. A* 370 (2012) 689–714.
- [36] G.T. Kalghatgi, Developments in internal combustion engines and implications for combustion science and future transport fuels, *Proc. Combust. Inst.* 35 (2015) 101–115.
- [37] L. Bates, D. Bradley, G. Paczko, N. Peters, Engine hot spots: Modes of auto-ignition and reaction propagation, *Combust. Flame* 166 (2016) 80–85.
- [38] L. Bates, D. Bradley, I. Gorbatenko, A.S. Tomlin, Computation of methane/air ignition delay and excitation times, using comprehensive and reduced chemical mechanisms and their relevance in engine autoignition, *Combust. Flame* 185 (2017) 105–116.
- [39] A. Robert, J.-M. Zaccardi, C. Dul, A. Guerouani, J. Rudloff, Numerical study of auto-ignition propagation modes in toluene reference fuel–air mixtures: Toward a better understanding of abnormal combustion in spark-ignition engines, *Int. J. Engine Res.* (2018) 1–12.
- [40] J.Y. Pan, G.Q. Shu, H.Q. Wei, Interaction of flame propagation and pressure waves during knocking combustion in spark-ignition engines, *Combust. Sci. Technol.* 186 (2014) 192–209.
- [41] J.Y. Pan, H.Q. Wei, G.Q. Shu, Z. Chen, P. Zhao, The role of low temperature chemistry in combustion mode development under elevated pressures, *Combust. Flame* 174 (2016) 179–193.
- [42] L. Bates, D. Bradley, Deflagrative, auto-ignitive, and detonative propagation regimes in engines, *Combust. Flame* 175 (2017) 118–122.
- [43] T.H. Zhang, W.Q. Sun, Y.G. Ju, Multi-scale modeling of detonation formation with concentration and temperature gradients in n-heptane/air mixtures, *Proc. Combust. Inst.* 36 (2017) 1539–1547.
- [44] A. Guerouani, A. Robert, J.-M. Zaccardi, Detonation peninsula for TRF-air mixtures: assessment for the analysis of auto-ignition events in spark-ignition engines, *SAE Technical Paper* 2018-01-1721 (2018), doi:10.4271/2018-4201-1721.

- [45] H. Yu, Z. Chen, End-gas autoignition and detonation development in a closed chamber, *Combust. Flame* 162 (2015) 4102–4111.
- [46] H. Yu, C.K. Qi, Z. Chen, Effects of flame propagation speed and chamber size on end-gas autoignition, *Proc. Combust. Inst.* 36 (2017) 3533–3541.
- [47] H. Terashima, M. Koshi, Mechanisms of strong pressure wave generation in end-gas autoignition during knocking combustion, *Combust. Flame* 162 (2015) 1944–1956.
- [48] H. Terashima, A. Matsugi, M. Koshi, Origin and reactivity of hot-spots in end-gas autoignition with effects of negative temperature coefficients: relevance to pressure wave developments, *Combust. Flame* 184 (2017) 324–334.
- [49] J. Pan, G. Shu, P. Zhao, H. Wei, Z. Chen, Interactions of flame propagation, auto-ignition and pressure wave during knocking combustion, *Combust. Flame* 164 (2016) 319–328.
- [50] J.Y. Pan, H.Q. Wei, G.Q. Shu, R. Chen, Effect of pressure wave disturbance on auto-ignition mode transition and knocking intensity under enclosed conditions, *Combust. Flame* 185 (2017) 63–74.
- [51] H.Q. Wei, C.Y. Chen, G.Q. Shu, X.Y. Liang, L. Zhou, Pressure wave evolution during two hotspots autoignition within end-gas region under internal combustion engine-relevant conditions, *Combust. Flame* 189 (2018) 142–154.
- [52] L. Zander, G. Tornow, R. Klein, N. Djordjevic, Influence of autoignition delay time characteristics of different fuels on pressure, *Active flow and combustion control* 2018, Springer, Cham, 2019, pp. 151–166.
- [53] S.L. Liu, J.C. Hewson, J.H. Chen, H. Pitsch, Effects of strain rate on high-pressure nonpremixed n-heptane autoignition in counterflow, *Combust. Flame* 137 (2004) 320–339.
- [54] Z. Chen, M.P. Burke, Y.G. Ju, Effects of Lewis number and ignition energy on the determination of laminar flame speed using propagating spherical flames, *Proc. Combust. Inst.* 32 (2009) 1253–1260.
- [55] Z. Chen, Effects of radiation and compression on propagating spherical flames of methane/air mixtures near the lean flammability limit, *Combust. Flame* 157 (2010) 2267–2276.
- [56] M. Sun, K. Takayama, Conservative smoothing on an adaptive quadrilateral grid, *J. Comput. Phys.* 150 (1999) 143–180.
- [57] S.Z. Chen, K. Xu, C. Lee, Q.D. Cai, A unified gas kinetic scheme with moving mesh and velocity space adaptation, *J. Comput. Phys.* 231 (2012) 6643–6664.